Looking for axions in exotic, highly magnetised White Dwarf stars

Ruben Zatini

IAC - Instituto de Astrofísica de Canarias
LAPTh/CNRS - Laboratoire d'Annecy-le-Vieux de Physique Théorique

October 8, 2024

Funded by the European Union

Education

Università degli Studi di Padova, MSc in Physics of the Fundamental Interactions
Looking for axions in exotic, highly magnetised White Dwarf stars
Supervised by Luca Di Luzio, Sebastian Hoof

KU Leuven, Study Abroad: Erasmus+ student

Università degli Studi di Firenze, BSc in Physics and Astrophysics
On the gravitational interaction of two massless particles
Supervised by Dimitri Colferai

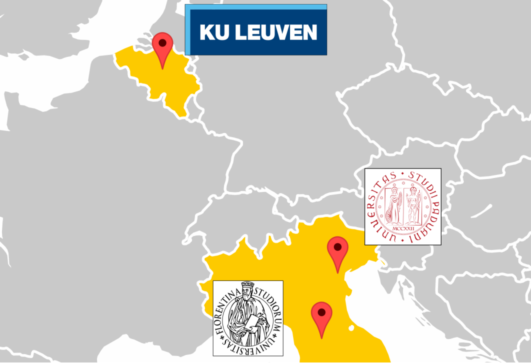

Joint PhD project

Instituto de Astrofísica de Canarias - IAC
Supervised by Jorge Martin Camalich
Laboratoire d'Annecy-le-Vieux de Physique Théorique - LAPTh/CNRS
Supervised by Francesca Calore

Probing light dark sectors in extreme astrophysical objects

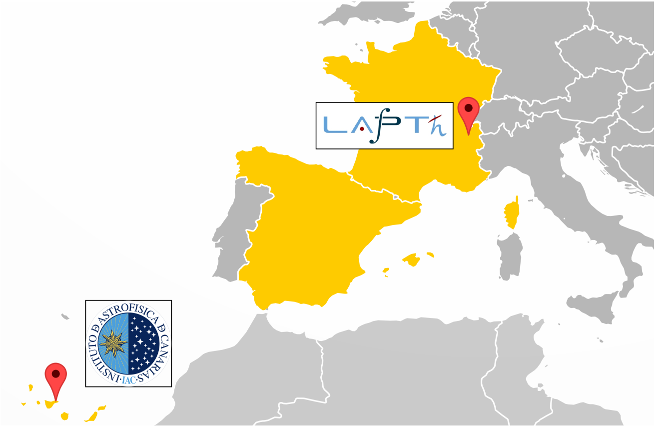

Theoretical motivations and phenomenology

- The strong CP problem: absence of CP violation in strong interactions
  $\Rightarrow$ The QCD axion emerges as a by product of a mechanism solving this fundamental puzzle of particle physics

Theoretical motivations and phenomenology

- The strong CP problem: absence of CP violation in strong interactions
  $\Rightarrow$ The QCD axion emerges as a by product of a mechanism solving this fundamental puzzle of particle physics

- Axions can also explain Dark Matter abundance in the Universe

Theoretical motivations and phenomenology

- The strong CP problem: absence of CP violation in strong interactions
  $\Rightarrow$ The QCD axion emerges as a by product of a mechanism solving this fundamental puzzle of particle physics

- Axions can also explain Dark Matter abundance in the Universe

Axion mass and interactions with SM particles: $m_a,\, g_a^{\rm SM} \propto 1/f_a$
Experiments imply a large value of $f_a \Rightarrow$ axion is light and weakly-interacting
$\Rightarrow$ It can be produced in astrophysical environments and escape without being reabsorbed

Theoretical motivations and phenomenology

- The strong CP problem: absence of CP violation in strong interactions
  $\Rightarrow$ The QCD axion emerges as a by product of a mechanism solving this fundamental puzzle of particle physics

- Axions can also explain Dark Matter abundance in the Universe

Axion mass and interactions with SM particles: $m_a,\, g_a^{\rm SM} \propto 1/f_a$
Experiments imply a large value of $f_a \Rightarrow$ axion is light and weakly-interacting
$\Rightarrow$ It can be produced in astrophysical environments and escape without being reabsorbed

Thesis phenomenology: axion production inside white dwarfs and subsequent conversion into X-ray photons inside their magnetosphere

$\Rightarrow$ g_{aee} and $g_{a\gamma\gamma}$ are the most important couplings

Axion phenomenology in WDs

g_{aee} enables axion emission through *bremsstrahlung*:

$$e^- + (A, Z) \rightarrow e^- + (A, Z) + a$$

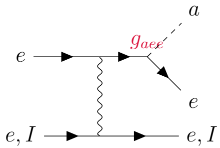

Axion phenomenology in WDs

g_{aee} enables axion emission through *bremsstrahlung*:

$$e^- + (A, Z) \rightarrow e^- + (A, Z) + a$$

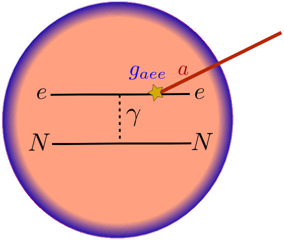

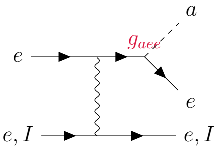

g_{aee} enables axion emission through *bremsstrahlung*:

$$e^- + (A, Z) \to e^- + (A, Z) + a$$

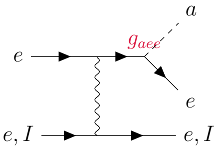

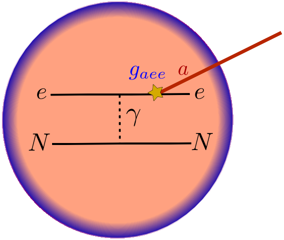

Phenomenological consequence:

Axion conversion into detectable photons in the B-field of the WD $\Rightarrow$ axion indirect detection

Axion phenomenology in WDs

g_{aee} enables axion emission through *bremsstrahlung*:

$$e^- + (A, Z) \rightarrow e^- + (A, Z) + a$$

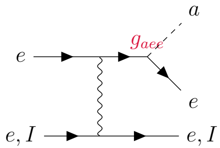

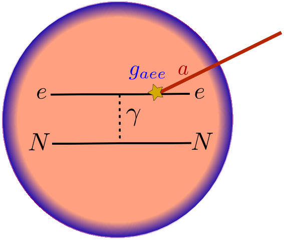

Phenomenological consequence:

Axion conversion into detectable photons in the B-field of the WD ⇒ axion indirect detection

$g_{a\gamma\gamma}$ mediates axion-photon oscillation through *Inverse Primakoff* process ⇒ X-ray emission

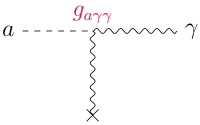

Axion phenomenology in WDs

g_{aee} enables axion emission through *bremsstrahlung*:

$$e^- + (A, Z) \to e^- + (A, Z) + a$$

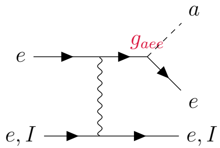

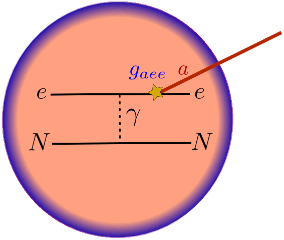

Phenomenological consequence:

Axion conversion into detectable photons in the B-field of the WD ⇒ axion indirect detection

$g_{a\gamma\gamma}$ mediates axion-photon oscillation through *Inverse Primakoff* process ⇒ X-ray emission

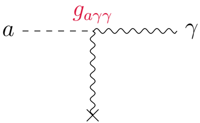

WDs are not expected to emit X-ray photons ⇒ clean environment for detection [Bilikova et al. (2010)]

Aims of the work

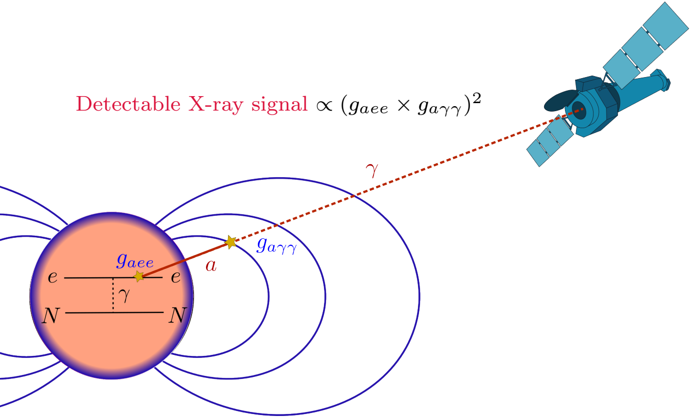

Aims of the work

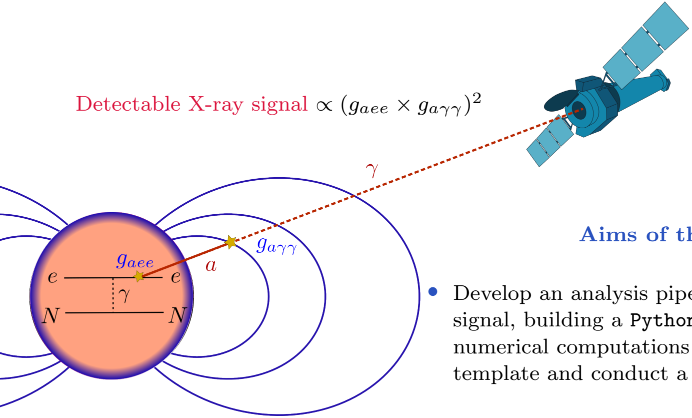

Aims of the work:

- Develop an analysis pipeline for this type of X-ray signal, building a `Python` framework to perform numerical computations for construct a signal template and conduct a statistical analysis

Detectable X-ray signal $\propto (g_{aee} \times g_{a\gamma\gamma})^2$

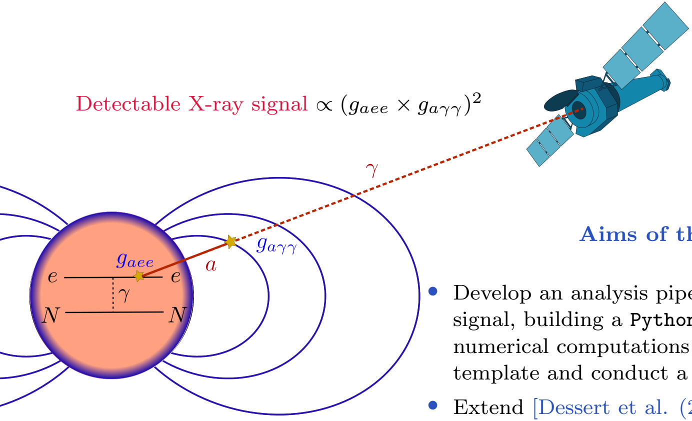

Aims of the work:

- Develop an analysis pipeline for this type of X-ray signal, building a `Python` framework to perform numerical computations for construct a signal template and conduct a statistical analysis
- Extend [Dessert et al. (2019, '22)]

Aims of the work

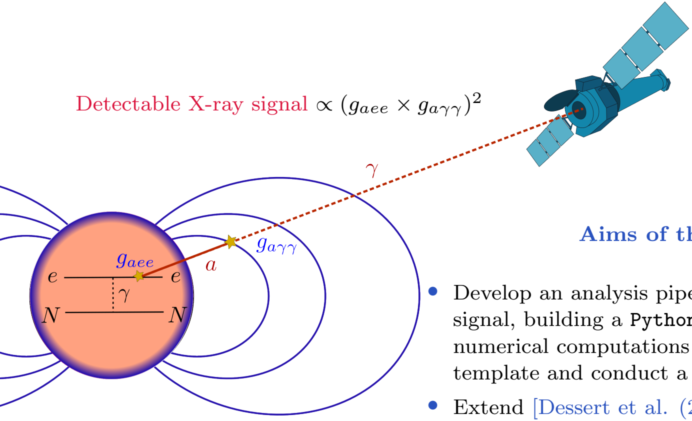

Aims of the work:

- Develop an analysis pipeline for this type of X-ray signal, building a `Python` framework to perform numerical computations for construct a signal template and conduct a statistical analysis
- Extend [Dessert et al. (2019, '22)]
- Provide an application to *Chandra* observation of MWD RE J0317-853 $\Rightarrow$ bound on $g_{a\gamma\gamma} \times g_{aee}$

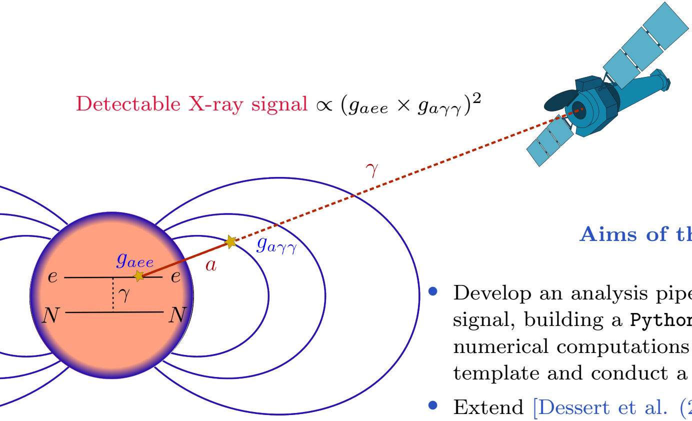

Aims of the work:

- Develop an analysis pipeline for this type of X-ray signal, building a `Python` framework to perform numerical computations for construct a signal template and conduct a statistical analysis
- Extend [Dessert et al. (2019, '22)]
- Provide an application to *Chandra* observation of MWD RE J0317-853 $\Rightarrow$ bound on $g_{a\gamma\gamma} \times g_{aee}$
- Assess the impact of different background models

Axion emission in WDs

Axion bremsstrahlung emissivity and luminosity:

$$\frac{d\varepsilon_a}{d\omega} = \frac{\alpha_{EM}^2 g_{aee}^2}{4\pi^3 m_e^2} \frac{\omega^3}{e^{\omega/T} - 1} \sum_s \frac{Z_s^2 \rho_s F_s}{A_s u} \quad \Rightarrow \quad \frac{dL_\mathrm{a}}{d\omega}(\omega) = 4\pi \int_0^{\mathrm{R_{WD}}} dr r^2 \frac{d\varepsilon_a}{d\omega}(r)$$

Plasma effects are described by F_s **factors**: for WD cores numerically computed

Axion emission in WDs

Axion bremsstrahlung emissivity and luminosity:

$$\frac{d\varepsilon_a}{d\omega} = \frac{\alpha_{EM}^2 g_{aee}^2}{4\pi^3 m_e^2} \frac{\omega^3}{e^{\omega/T}-1} \sum_s \frac{Z_s^2 \rho_s F_s}{A_s u} \quad \Rightarrow \quad \frac{dL_{\mathrm{a}}}{d\omega}(\omega) = 4\pi \int_0^{\mathrm{R_{WD}}} dr r^2 \frac{d\varepsilon_a}{d\omega}(r)$$

Plasma effects are described by F_s **factors**: for WD cores numerically computed

Need a **WD modeling**: density and composition profiles + core temperature

Axion emission in WDs

Axion bremsstrahlung emissivity and luminosity:

$$\frac{d\varepsilon_a}{d\omega} = \frac{\alpha_{EM}^2 g_{aee}^2}{4\pi^3 m_e^2} \frac{\omega^3}{e^{\omega/T}-1} \sum_s \frac{Z_s^2 \rho_s F_s}{A_s u} \quad \Rightarrow \quad \frac{dL_a}{d\omega}(\omega) = 4\pi \int_0^{R_{WD}} dr r^2 \frac{d\varepsilon_a}{d\omega}(r)$$

Plasma effects are described by F_s **factors**: for WD cores numerically computed

Need a **WD modeling**: density and composition profiles + core temperature

Application to **RE J0317-853**

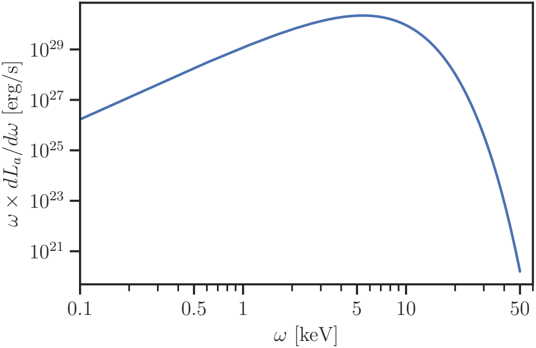

Axion-photon conversion

Axion electrodynamics: system of equations that mixes axions and photons
[Raffelt & Stodolsky (1988); Millar et al. (2017)]

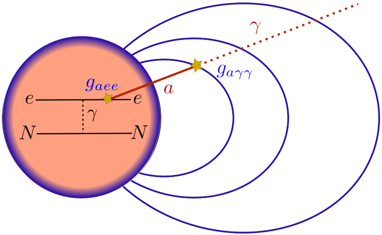

$$\left[i\partial_r + \omega + \begin{pmatrix} \Delta_\parallel & \Delta_B \\ \Delta_B & \Delta_a \end{pmatrix}\right]\begin{pmatrix} A_\parallel \\ a \end{pmatrix} = 0$$

Axion-photon conversion

Axion electrodynamics: system of equations that mixes axions and photons
[Raffelt & Stodolsky (1988); Millar et al. (2017)]

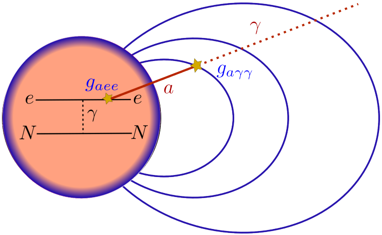

$$\left[i\partial_r + \omega + \begin{pmatrix} \Delta_\parallel & \Delta_B \\ \Delta_B & \Delta_a \end{pmatrix}\right]\begin{pmatrix} A_\parallel \\ a \end{pmatrix} = 0$$

In weak-mixing limit:

$$p_{a\to\gamma} = \left| \int_{\mathrm{R_{WD}}}^{\infty} dr' \Delta_B(r') e^{i\Delta_a r' - i\int_{R_{\mathrm{WD}}}^{r'} dr'' \Delta_\parallel(r'')} \right|^2$$

Axion-photon conversion

Axion electrodynamics: system of equations that mixes axions and photons
[Raffelt & Stodolsky (1988); Millar et al. (2017)]

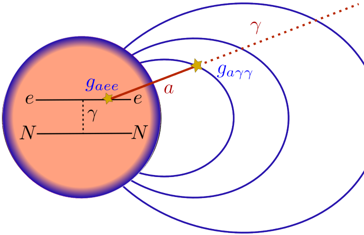

$$\left[i\partial_r + \omega + \begin{pmatrix} \Delta_\parallel & \Delta_B \\ \Delta_B & \Delta_a \end{pmatrix}\right] \begin{pmatrix} A_\parallel \\ a \end{pmatrix} = 0$$

In weak-mixing limit:

$$p_{\mathrm{a}\to\gamma} = \left| \int_{\mathrm{R_{WD}}}^{\infty} dr' \Delta_B(r') e^{i\Delta_a r' - i\int_{R_{\mathrm{WD}}}^{r'} dr'' \Delta_\parallel(r'')} \right|^2$$

- Dependence on magnetic field geometry

Axion-photon conversion

Axion electrodynamics: system of equations that mixes axions and photons
[Raffelt & Stodolsky (1988); Millar et al. (2017)]

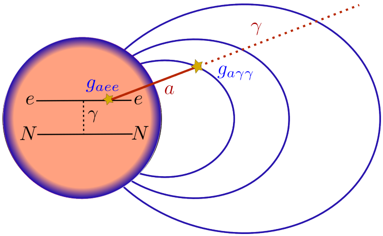

$$\left[i\partial_r + \omega + \begin{pmatrix} \Delta_\parallel & \Delta_B \\ \Delta_B & \Delta_a \end{pmatrix}\right] \begin{pmatrix} A_\parallel \\ a \end{pmatrix} = 0$$

In weak-mixing limit:

$$p_{\mathrm{a}\to\gamma} = \left| \int_{\mathrm{R_{WD}}}^{\infty} dr' \Delta_B(r') e^{i\Delta_a r' - i\int_{R_{\mathrm{WD}}}^{r'} dr'' \Delta_\parallel(r'')} \right|^2$$

- Dependence on magnetic field geometry ⇒ magnetic dipole field
[Burleigh et al. (1999)]

Axion-photon conversion

Axion electrodynamics: system of equations that mixes axions and photons
[Raffelt & Stodolsky (1988); Millar et al. (2017)]

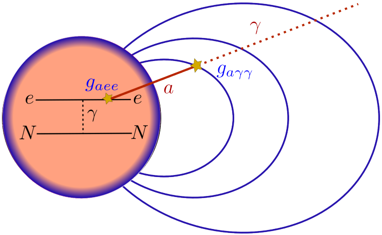

$$\left[i\partial_r + \omega + \begin{pmatrix} \Delta_\parallel & \Delta_B \\ \Delta_B & \Delta_a \end{pmatrix}\right]\begin{pmatrix} A_\parallel \\ a \end{pmatrix} = 0$$

In weak-mixing limit:

$$p_{a\to\gamma} = \left| \int_{R_{WD}}^{\infty} dr' \Delta_B(r') e^{i\Delta_a r' - i\int_{R_{WD}}^{r'} dr'' \Delta_\parallel(r'')} \right|^2$$

- Dependence on magnetic field geometry ⇒ magnetic dipole field
  [Burleigh et al. (1999)]
- Dependence on the axion mass:

Axion-photon conversion

Axion electrodynamics: system of equations that mixes axions and photons
[Raffelt & Stodolsky (1988); Millar et al. (2017)]

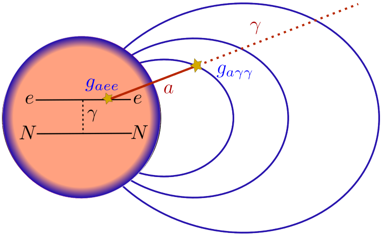

$$\left[i\partial_r + \omega + \begin{pmatrix} \Delta_\parallel & \Delta_B \\ \Delta_B & \Delta_a \end{pmatrix}\right]\begin{pmatrix} A_\parallel \\ a \end{pmatrix} = 0$$

In weak-mixing limit:

$$p_{a\to\gamma} = \left| \int_{\mathrm{R_{WD}}}^{\infty} dr' \Delta_B(r') e^{i\Delta_a r' - i\int_{\mathrm{R_{WD}}}^{r'} dr'' \Delta_\parallel(r'')} \right|^2$$

- Dependence on magnetic field geometry $\Rightarrow$ magnetic dipole field
  [Burleigh et al. (1999)]
- Dependence on the axion mass: focus on low-mass limit $m_a \to 0$ which gives a sizable $p_{a\to\gamma}$, good approximation for axions with $m_a \ll 10^{-5}\,\mathrm{eV}$

Axion-photon conversion

Axion electrodynamics: system of equations that mixes axions and photons
[Raffelt & Stodolsky (1988); Millar et al. (2017)]

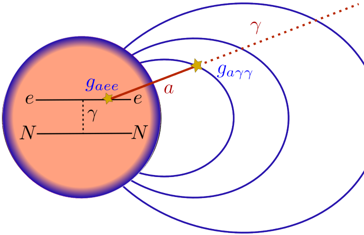

$$\left[i\partial_r + \omega + \begin{pmatrix} \Delta_\parallel & \Delta_B \\ \Delta_B & \Delta_a \end{pmatrix}\right]\begin{pmatrix} A_\parallel \\ a \end{pmatrix} = 0$$

In weak-mixing limit:

$$p_{a\to\gamma} = \left| \int_{R_{WD}}^{\infty} dr' \Delta_B(r') e^{i\Delta_a r' - i\int_{R_{WD}}^{r'} dr'' \Delta_\parallel(r'')} \right|^2$$

- Dependence on magnetic field geometry $\Rightarrow$ magnetic dipole field
  [Burleigh et al. (1999)]
- Dependence on the axion mass: focus on low-mass limit $m_a \to 0$ which gives a sizable $p_{a\to\gamma}$, good approximation for axions with $m_a \ll 10^{-5}\,\text{eV}$

Application to **RE J0317-853**: $p_{a\to\gamma} \sim \mathcal{O}(10^{-4}) \times \left(\frac{g_{a\gamma\gamma}}{10^{-11}\ \text{GeV}^{-1}}\right)^2$

Axion-induced X-ray flux prediction

$$\frac{dF_{\gamma_a}}{d\omega} \propto \frac{dL_a}{d\omega}(\omega) \times p_{a\to\gamma}(\omega) \propto g_{aee}^2 \times g_{a\gamma\gamma}^2$$

Axion-induced X-ray flux prediction

$$\frac{dF_{\gamma_a}}{d\omega} \propto \frac{dL_a}{d\omega}(\omega) \times p_{a\to\gamma}(\omega) \propto g_{aee}^2 \times g_{a\gamma\gamma}^2$$

Application to **RE J0317-853:**

Axion-induced X-ray flux prediction

$$\frac{dF_{\gamma_a}}{d\omega} \propto \frac{dL_a}{d\omega}(\omega) \times p_{a\to\gamma}(\omega) \propto g_{aee}^2 \times g_{a\gamma\gamma}^2$$

Application to **RE J0317-853:**

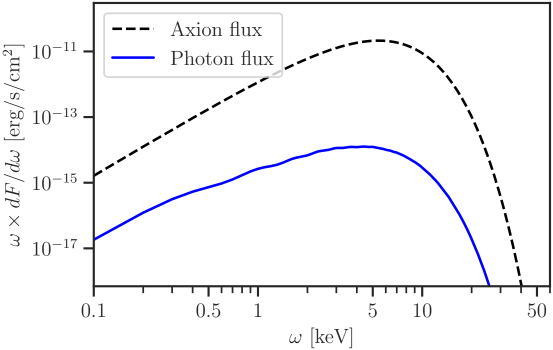

$\Rightarrow$ The X-ray signal peaks in the keV range, with its intensity modulated by a signal parameter $\theta_s \propto (g_{aee} \times g_{a\gamma\gamma})^2$

Observation of RE J0317-853 and analysis

Chandra observation: 37.42 ks

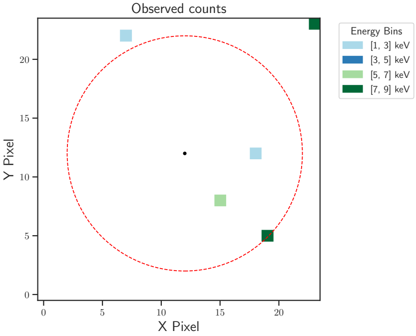

Implement *Chandra* response functions

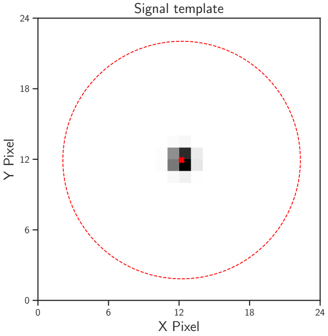

Observation of RE J0317-853 and analysis

Chandra observation: 37.42 ks

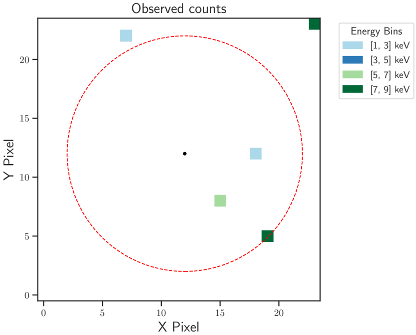

Implement *Chandra* response functions

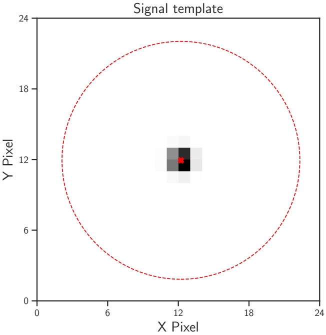

$$L(\boldsymbol{\theta}) = \prod_{i=1}^{4} \prod_{j=1}^{N_{\rm pix}} \frac{\mu_{i,j}(\boldsymbol{\theta})^{n_{i,j}} e^{-\mu_{i,j}(\boldsymbol{\theta})}}{n_{i,j}!} \quad \text{with} \quad \mu_{i,j}(\boldsymbol{\theta}) = s_{i,j}(\theta_s) + b_{i,j}(\boldsymbol{\theta}_b)$$

Observation of RE J0317-853 and analysis

Chandra observation: 37.42 ks

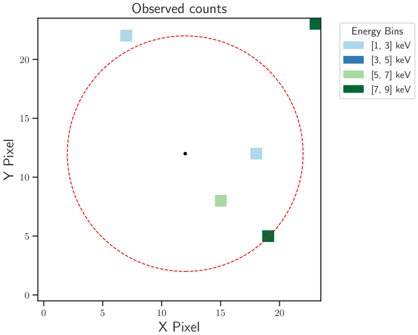

Implement *Chandra* response functions

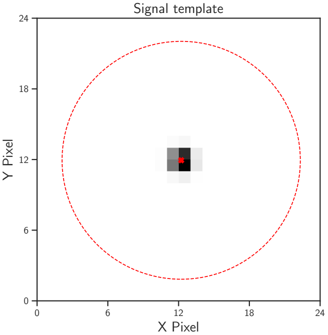

$$L(\boldsymbol{\theta}) = \prod_{i=1}^{4} \prod_{j=1}^{N_{\text{pix}}} \frac{\mu_{i,j}(\boldsymbol{\theta})^{n_{i,j}} e^{-\mu_{i,j}(\boldsymbol{\theta})}}{n_{i,j}!} \quad \text{with} \quad \mu_{i,j}(\boldsymbol{\theta}) = s_{i,j}(\theta_s) + b_{i,j}(\boldsymbol{\theta}_b)$$

Employing different background models, compute profile likelihood for θ_s $\Rightarrow$ determine an upper limit on the product of the couplings $g_{aee} \times g_{a\gamma\gamma}$

Statistical analysis

Implement different background models

- **Free** background: Four parameters, one in each energy bin, rescaling the background spatial template
- **Constant** background: Single parameter for all energy bins and pixels
- **Linear** background: Background described by a linear spectrum
- **Power-law** background: Background described by a power law spectrum

$$\frac{dN_{\rm bkg}}{d\omega} = K \cdot \left(\frac{\omega}{\omega_0}\right)^{-\alpha}$$

physically well-motivated, possible astrophysical background due to accretion or binary companion ⇒ X-ray emission [Kluzniak et al. (1989)]

Statistical analysis

Implement different background models

- **Free** background: Four parameters, one in each energy bin, rescaling the background spatial template
- **Constant** background: Single parameter for all energy bins and pixels
- **Linear** background: Background described by a linear spectrum
- **Power-law** background: Background described by a power law spectrum

$$\frac{dN_{\rm bkg}}{d\omega} = K \cdot \left(\frac{\omega}{\omega_0}\right)^{-\alpha}$$

physically well-motivated, possible astrophysical background due to accretion or binary companion ⇒ X-ray emission [Kluzniak et al. (1989)]

Little impact on the analysis, free background for consistency with [Dessert et al. 2022]

$$g_{aee} \times g_{a\gamma\gamma} < 2.3 \times 10^{-25}\,\text{GeV}^{-1} \quad (2\sigma) \quad \text{This thesis}$$

$$g_{aee} \times g_{a\gamma\gamma} < 1.3 \times 10^{-25}\,\text{GeV}^{-1} \quad (2\sigma) \quad \text{[Dessert et al. 2022]}$$

⇒ Dessert et al. obtained a stronger bound by a factor ~ 1.7

Summary

Axion emission from white dwarfs will induce a hard X-ray signature. **[Dessert, Long, & Safdi (2019)]** **[Dessert, Long, & Safdi (2022)]**

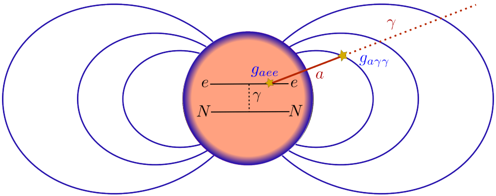

Summary

Axion emission from white dwarfs will induce a hard X-ray signature. **[Dessert, Long, & Safdi (2019)]** **[Dessert, Long, & Safdi (2022)]**

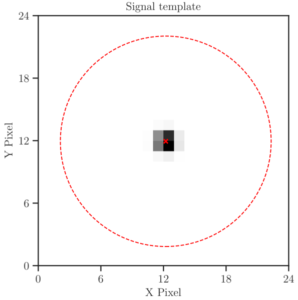

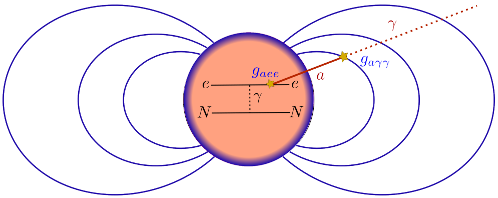

Development of an analysis pipeline for this type of signal: **Construct of a signal template and provide an application for RE J0317-853**

Summary

Axion emission from white dwarfs will induce a hard X-ray signature. [Dessert, Long, & Safdi (2019)] [Dessert, Long, & Safdi (2022)]

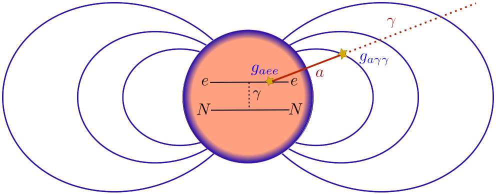

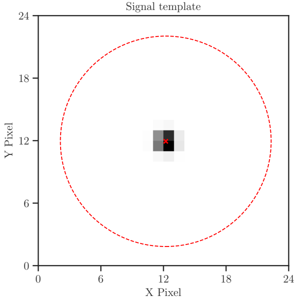

Development of an analysis pipeline for this type of signal: **Construct of a signal template and provide an application for RE J0317-853**

No evidence of X-ray emission from *Chandra* observation of RE J0317-853: **Strong limit on axion couplings and quantify the impact of different background models**

$\Rightarrow g_{aee} \times g_{a\gamma\gamma} < 2.3 \times 10^{-25}\ \mathrm{GeV}^{-1}\ (2\sigma)$ in line with [Dessert et al. (2022)]

Outlook and improvements

- Apply the analysis to various axion models
  $\Rightarrow$ which ones can be constrained more than others with WDs observations?

- Extend the analysis to processes mediated by other couplings
  $\Rightarrow$ ^{57}Fe de-excitation via axion-nucleon coupling

- Refine the computation of F factors
  $\Rightarrow$ Numerical parametrization available in literature is not totally adequate

Backup slide: medium factors F_s

Axion bremsstrahlung emissivity spectrum:

$$\frac{d\varepsilon_a}{d\omega} = \frac{\alpha_{\mathrm{EM}}^2 g_{aee}^2}{4\pi^3 m_e^2} \frac{\omega^3}{e^{\omega/T} - 1} \sum_s \frac{Z_s^2 \rho_s F_s}{A_s m_u}$$

Backup slide: medium factors F_s

Axion bremsstrahlung emissivity spectrum:

$$\frac{d\varepsilon_a}{d\omega} = \frac{\alpha_{\mathrm{EM}}^2 g_{aee}^2}{4\pi^3 m_e^2} \frac{\omega^3}{e^{\omega/T} - 1} \sum_s \frac{Z_s^2 \rho_s}{A_s m_u} F$$

Backup slide: medium factors F_s

Axion bremsstrahlung emissivity spectrum:

$$\frac{d\varepsilon_a}{d\omega} = \frac{\alpha_{\rm EM}^2 g_{aee}^2}{4\pi^3 m_e^2} \frac{\omega^3}{e^{\omega/T} - 1} \sum_s \frac{Z_s^2 \rho_s}{A_s m_u} F$$

Formal expression for F from axion emissivity calculation

$$F = \int \frac{d\Omega_2}{4\pi} \int \frac{d\Omega_a}{4\pi} \frac{(1-\beta_F^2)[2(1-c_{12}) - (c_{1a} - c_{2a})^2]}{(1-c_{1a}\beta_F)(1-c_{2a}\beta_F)(1-c_{12})(1-c_{12}+\kappa_{\rm s})}$$

in weakly coupled plasma

Backup slide: medium factors F_s

Axion bremsstrahlung emissivity spectrum:

$$\frac{d\varepsilon_a}{d\omega} = \frac{\alpha_{\rm EM}^2 g_{aee}^2}{4\pi^3 m_e^2} \frac{\omega^3}{e^{\omega/T}-1} \sum_s \frac{Z_s^2 \rho_s}{A_s m_u} F$$

Formal expression for F from axion emissivity calculation

$$F = \int \frac{d\Omega_2}{4\pi} \int \frac{d\Omega_a}{4\pi} \frac{(1-\beta_F^2)[2(1-c_{12})-(c_{1a}-c_{2a})^2]}{(1-c_{1a}\beta_F)(1-c_{2a}\beta_F)(1-c_{12})(1-c_{12}+\kappa_{\rm s})}$$

in weakly coupled plasma

WD plasma is strongly coupled $\Rightarrow$ Numerical parametrization is needed

AXION BREMSSTRAHLUNG IN DENSE STARS. II. PHONON CONTRIBUTIONS
MASAYUKI NAKAGAWA, TOMOO ADACHI, YASUHARU KOHYAMA, AND NAOKI ITOH
Department of Physics, Sophia University, Tokyo, Japan
Received 1987 June 22; accepted 1987 August 21

Only for WD composed by a single element
$\Rightarrow$ compute different F_s and then sum up

Backup slide: medium factors F_s

Axion bremsstrahlung emissivity spectrum:

$$\frac{d\varepsilon_a}{d\omega} = \frac{\alpha_{\rm EM}^2 g_{aee}^2}{4\pi^3 m_e^2} \frac{\omega^3}{e^{\omega/T}-1} \sum_s \frac{Z_s^2 \rho_s}{A_s m_u} F$$

Formal expression for F from axion emissivity calculation

$$F = \int \frac{d\Omega_2}{4\pi} \int \frac{d\Omega_a}{4\pi} \frac{(1-\beta_F^2)[2(1-c_{12})-(c_{1a}-c_{2a})^2]}{(1-c_{1a}\beta_F)(1-c_{2a}\beta_F)(1-c_{12})(1-c_{12}+\kappa_{\rm s})}$$

in weakly coupled plasma

WD plasma is strongly coupled $\Rightarrow$ Numerical parametrization is needed

AXION BREMSSTRAHLUNG IN DENSE STARS. II. PHONON CONTRIBUTIONS
MASAYUKI NAKAGAWA, TOMOO ADACHI, YASUHARU KOHYAMA, AND NAOKI ITOH
Department of Physics, Sophia University, Tokyo, Japan
Received 1987 June 22; accepted 1987 August 21

Only for WD composed by a single element
$\Rightarrow$ compute different F_s and then sum up

But F is not linear on the species, a unified procedure to treat multiple elements is needed!

Backup slide: Parameter space

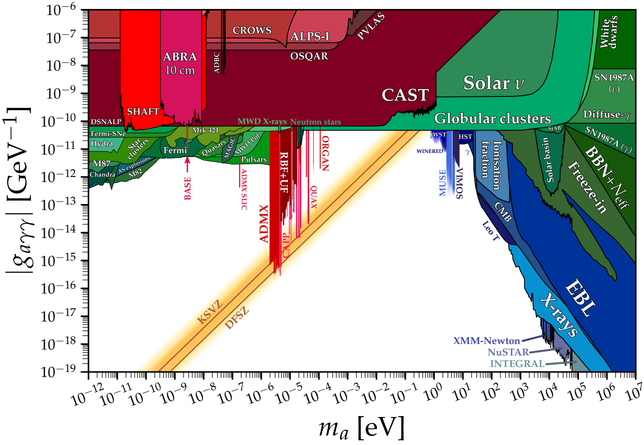

Backup slide: Parameter space

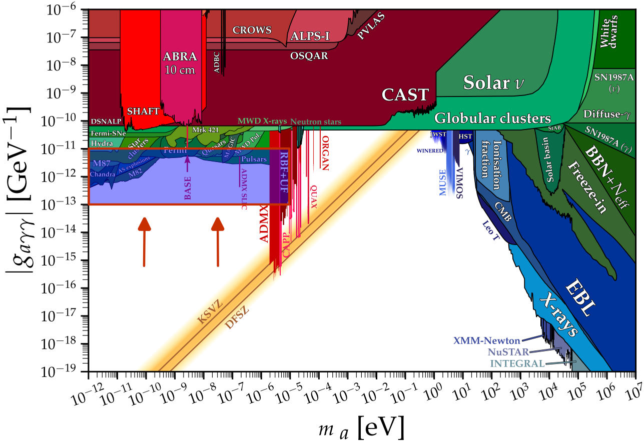

⇒ ALPs: no restriction, they can lie everywhere in the parameter space

Backup slide: $p_{\mathrm{a}\to\gamma}$ computation

Axion-photon conversion probability:

$$p_{\mathrm{a}\to\gamma} = \left| \int_{\mathrm{R_{WD}}}^{\infty} dr' \Delta_B(r') e^{i\Delta_a r' - i\int_{R_{\mathrm{WD}}}^{r'} dr'' \Delta_{\parallel}(r'')} \right|^2 .$$

Backup slide: $p_{\mathrm{a}\to\gamma}$ computation

Axion-photon conversion probability:

$$p_{\mathrm{a}\to\gamma} = \left| \int_{\mathrm{R_{WD}}}^{\infty} dr' \Delta_B(r') e^{i\Delta_a r' - i\int_{\mathrm{R_{WD}}}^{r'} dr'' \Delta_{\parallel}(r'')} \right|^2 .$$

$p_{\mathrm{a}\to\gamma}(\theta)$, with θ the angle between axion radial trajectory $\hat{r}$ and magnetic axis $\hat{m}$.
Dipole field + viewing angle and $\hat{m}$ misalignment: [Burleigh et al. (1999)]

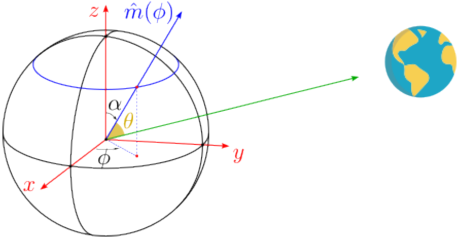

Backup slide: $p_{a\to\gamma}$ computation

Axion-photon conversion probability:

$$p_{a\to\gamma} = \left| \int_{R_{WD}}^{\infty} dr' \Delta_B(r') e^{i\Delta_a r' - i\int_{R_{WD}}^{r'} dr'' \Delta_{\parallel}(r'')} \right|^2.$$

$p_{a\to\gamma}(\theta)$, with θ the angle between axion radial trajectory $\hat{r}$ and magnetic axis $\hat{m}$.
Dipole field + viewing angle and $\hat{m}$ misalignment: [Burleigh et al. (1999)]

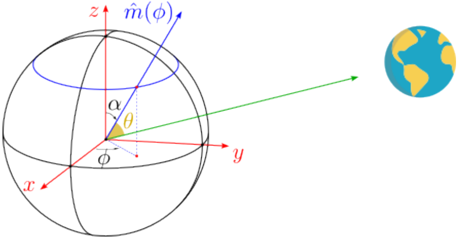

What value of θ should we take?

Backup slide: $p_{\mathrm{a}\to\gamma}$ computation

Axion-photon conversion probability:

$$p_{\mathrm{a}\to\gamma} = \left| \int_{\mathrm{R_{WD}}}^{\infty} dr' \Delta_B(r') e^{i\Delta_a r' - i\int_{\mathrm{R_{WD}}}^{r'} dr'' \Delta_{\parallel}(r'')} \right|^2 .$$

$p_{\mathrm{a}\to\gamma}(\theta)$, with θ the angle between axion radial trajectory $\hat{r}$ and magnetic axis $\hat{m}$.
Dipole field + viewing angle and $\hat{m}$ misalignment: [Burleigh et al. (1999)]

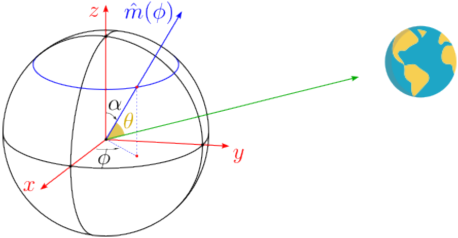

What value of θ should we take?
$\Rightarrow$ Observation time $\sim 40\,\mathrm{ks} \gg\sim 700\,\mathrm{s}$ rotational period of RE J0317-853

Backup slide: $p_{\mathrm{a}\to\gamma}$ computation

Generate trajectory with uniformly distributed ϕ

Backup slide: $p_{\mathrm{a}\to\gamma}$ computation

Generate trajectory with uniformly distributed ϕ + parametrization of $\theta = \theta(\phi)$

Backup slide: $p_{\mathrm{a}\to\gamma}$ computation

Generate trajectory with uniformly distributed ϕ + parametrization of $\theta = \theta(\phi)$
$\Rightarrow$ compute $p_{\mathrm{a}\to\gamma}(\phi) = p_{\mathrm{a}\to\gamma}(\theta(\phi))$ and then average over ϕ:

$$\langle p_{\mathrm{a}\to\gamma}\rangle_\phi = \frac{1}{2\pi}\int_0^{2\pi} p_{\mathrm{a}\to\gamma}(\phi)d\phi \qquad \text{using } \texttt{np.trapz}$$

Backup slide: $p_{\mathrm{a}\to\gamma}$ computation

Generate trajectory with uniformly distributed ϕ + parametrization of $\theta = \theta(\phi)$
$\Rightarrow$ compute $p_{\mathrm{a}\to\gamma}(\phi) = p_{\mathrm{a}\to\gamma}(\theta(\phi))$ and then average over ϕ:

$$\langle p_{\mathrm{a}\to\gamma}\rangle_\phi = \frac{1}{2\pi}\int_0^{2\pi} p_{\mathrm{a}\to\gamma}(\phi)d\phi \qquad \text{using } \texttt{np.trapz}$$

Repeat the numerical integration for a range of energies $\omega \in [0, 50]\,\mathrm{keV}$
$\Rightarrow$ Construct energy profile for $p_{\mathrm{a}\to\gamma}(\omega)$

Backup slide: $p_{a\to\gamma}$ computation

Generate trajectory with uniformly distributed ϕ + parametrization of $\theta = \theta(\phi)$
$\Rightarrow$ compute $p_{a\to\gamma}(\phi) = p_{a\to\gamma}(\theta(\phi))$ and then average over ϕ:

$$\langle p_{a\to\gamma}\rangle_\phi = \frac{1}{2\pi}\int_0^{2\pi} p_{a\to\gamma}(\phi)d\phi \qquad \text{using } \texttt{np.trapz}$$

Repeat the numerical integration for a range of energies $\omega \in [0, 50]$ keV
$\Rightarrow$ Construct energy profile for $p_{a\to\gamma}(\omega)$

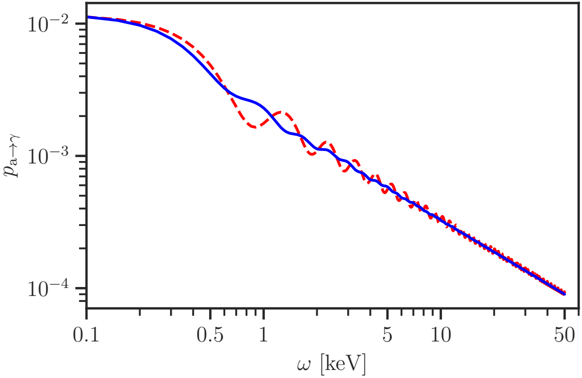

Backup slide: Statistical analysis

First type of analysis: utilize only spectral information

$$L(\boldsymbol{\theta}) = \prod_{i=1}^{4} \frac{\mu_i(\boldsymbol{\theta})^{n_i} e^{-\mu_i(\boldsymbol{\theta})}}{n_i!} \quad \text{with} \quad \mu_i(\boldsymbol{\theta}) = s_i(\theta_s) + b_i(\boldsymbol{\theta}_b),$$

and signal parameter $\theta_s \propto (g_{aee} \times g_{a\gamma\gamma})^2$

Backup slide: Statistical analysis

First type of analysis: utilize only spectral information

$$L(\boldsymbol{\theta}) = \prod_{i=1}^{4} \frac{\mu_i(\boldsymbol{\theta})^{n_i} e^{-\mu_i(\boldsymbol{\theta})}}{n_i!} \quad \text{with} \quad \mu_i(\boldsymbol{\theta}) = s_i(\theta_s) + b_i(\boldsymbol{\theta}_b),$$

and signal parameter $\theta_s \propto (g_{aee} \times g_{a\gamma\gamma})^2$

1. **Compute the best-fit parameters**: $\hat{\boldsymbol{\theta}} = \{\hat{\theta}_s, \hat{\boldsymbol{\theta}}_b\}$ by using `scipy.minimize` to perform a global minimization of

$$-\ln\left(L(\theta_s, \boldsymbol{\theta}_b)\right)$$

Backup slide: Statistical analysis

First type of analysis: utilize only spectral information

$$L(\boldsymbol{\theta}) = \prod_{i=1}^{4} \frac{\mu_i(\boldsymbol{\theta})^{n_i} e^{-\mu_i(\boldsymbol{\theta})}}{n_i!} \quad \text{with} \quad \mu_i(\boldsymbol{\theta}) = s_i(\theta_s) + b_i(\boldsymbol{\theta}_b),$$

and signal parameter $\theta_s \propto (g_{aee} \times g_{a\gamma\gamma})^2$

1. **Compute the best-fit parameters**: $\hat{\boldsymbol{\theta}} = \{\hat{\theta}_s, \hat{\boldsymbol{\theta}}_b\}$ by using `scipy.minimize` to perform a global minimization of

$$-\ln\left(L(\theta_s, \boldsymbol{\theta}_b)\right)$$

2. **Construct** $LLR(\theta_s)$ **profile for a range of hypothesized** θ_s:

$$LLR(\theta_s) = -2\ln\left(\frac{L(\theta_s, \hat{\hat{\boldsymbol{\theta}}}_b)}{L(\hat{\theta}_s, \hat{\boldsymbol{\theta}}_b)}\right)$$

where $\hat{\hat{\boldsymbol{\theta}}}_b$ are the background parameters optimized for a fixed value of θ_s.

Backup slide: Statistical analysis

First type of analysis: utilize only spectral information

$$L(\boldsymbol{\theta}) = \prod_{i=1}^{4} \frac{\mu_i(\boldsymbol{\theta})^{n_i} e^{-\mu_i(\boldsymbol{\theta})}}{n_i!} \quad \text{with} \quad \mu_i(\boldsymbol{\theta}) = s_i(\theta_s) + b_i(\boldsymbol{\theta}_b),$$

and signal parameter $\theta_s \propto (g_{aee} \times g_{a\gamma\gamma})^2$

1. **Compute the best-fit parameters**: $\hat{\boldsymbol{\theta}} = \{\hat{\theta}_s, \hat{\boldsymbol{\theta}}_b\}$ by using `scipy.minimize` to perform a global minimization of

   $$-\ln\left(L(\theta_s, \boldsymbol{\theta}_b)\right)$$

2. **Construct $LLR(\theta_s)$ profile for a range of hypothesized θ_s**:

   $$LLR(\theta_s) = -2\ln\left(\frac{L(\theta_s, \hat{\hat{\boldsymbol{\theta}}}_b)}{L(\hat{\theta}_s, \hat{\boldsymbol{\theta}}_b)}\right)$$

   where $\hat{\hat{\boldsymbol{\theta}}}_b$ are the background parameters optimized for a fixed value of θ_s.
3. **Determine the upper limit**: asymptotic formulae to constrain θ_s: we identify the value of θ_s at which the $LLR(\theta_s)$ crosses the 95% threshold

Backup slide: Statistical analysis

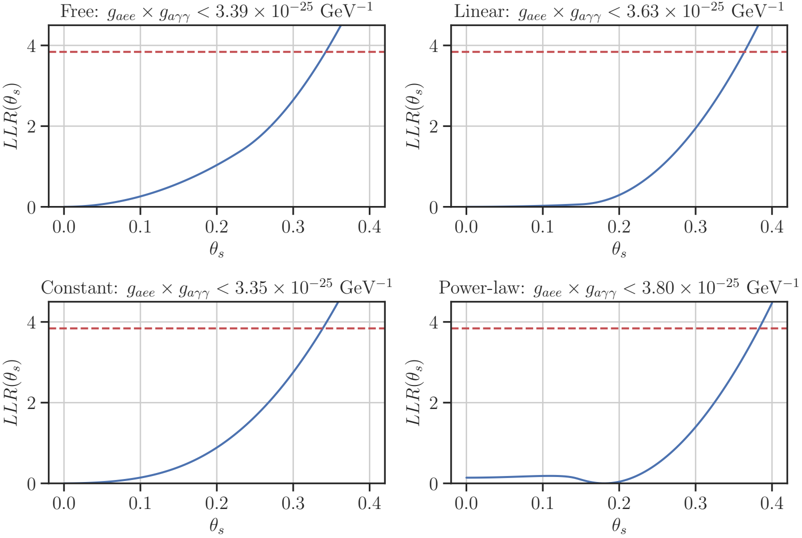

Backup slide: PQ symmetry

Realization of PQ symmetry in the UV is not unique; it requires colored PQ-charged fermions (quarks) for the color anomalous shift, replacing the $\bar{\theta}$-term with a dynamical field (the axion).

PQ-charged fermions can also be EM charged, leading to an EM anomalous term.
⇒ After SSB, the axion couples with photons and the PQ current:

$$\mathcal{L}_a \supset \frac{a}{v_{\rm PQ}} \frac{g_s^2 N}{16\pi^2} G^a_{\mu\nu} \widetilde{G}^{a\,\mu\nu} + \frac{a}{v_{\rm PQ}} \frac{e^2 E}{16\pi^2} F_{\mu\nu} \widetilde{F}^{\mu\nu} + \frac{\partial^\mu a}{v_{\rm PQ}} J^{\rm PQ}_\mu$$

Anomaly coefficients E, N and the fermionic PQ current vary by model:

- **Minimal KSVZ model:** PQ-charged fermions are heavy quarks, EM neutral ⇒ axion interacts only with gluons (*hadronic model*)
- **DFSZ model:** PQ-charged fermions include SM quarks and leptons ⇒ interaction with photons and electrons; $g_{a\gamma\gamma}$ and g_{aee} emerge already in the UV